Acta Crystallographica Section E
Structure Reports Online
ISSN 1600-5368

$Ba_{19}In_9N_9$, a subnitride containing isolated $[In_5]^{5-}$ and $[In_8]^{12-}$ Zintl anions

Hisanori Yamane,[a]* Shinya Sasaki,[b] Takashi Kajiwara,[c] Takahiro Yamada[a] and Masahiko Shimada[b]

[a]Center for Interdisciplinary Research, Tohoku University, 6-3 Aramaki, Aoba-ku, Sendai 980-8578, Japan, [b]Institute of Multidisciplinary Research for Advanced Materials, Tohoku University, 2-1-1 Katahira, Aoba-ku, Sendai 980-8577, Japan, and [c]Graduate School of Science, Department of Chemistry, Tohoku University, 6-3 Aramaki, Aoba-ku, Sendai 980-8578, Japan

Correspondence e-mail: yamane@cir.tohoku.ac.jp

Key indicators

Single-crystal X-ray study
T = 293 K
Mean σ(In–In) = 0.001 Å
R factor = 0.042
wR factor = 0.106
Data-to-parameter ratio = 35.6

For details of how these key indicators were automatically derived from the article, see http://journals.iucr.org/e.

Received 20 August 2004
Accepted 8 September 2004
Online 18 September 2004

Single crystals of nonadecabarium nonaindium nonanitride, $Ba_{19}In_9N_9$, were synthesized by the Na flux method under N_2 pressure. The compound crystallizes in the monoclinic space group $C2/m$, with Z = 2. Polyanionic indium clusters $[In_5]^{5-}$ and $[In_8]^{12-}$ are surrounded by Ba^{2+} cations and are located in a flat cage built of linked nitrogen-centred NBa_6 octahedra. The structural formula is expressed as $(Ba_{38}N_{18})[In_5]_2[In_8]$.

Comment

A wide variety of Zintl polyanions has been found in binary, ternary and multinary intermetallic compounds. Zintl polyanions of Ga and In are also contained in ternary and quaternary subnitrides, such as Sr_6Ga_5N, Ba_6Ga_5N (Cordier *et al.*, 1995), Ca_4In_2N, Sr_4In_2N (Cordier & Rönninger, 1987), $(Ba,Sr)_8Cu_3In_4N_5$ (Yamane, Sasaki, Kubota, Inoue *et al.*, 2002; Yamane *et al.*, 2003) and $Ba_{14}Cu_2In_4N_7$ (Yamane, Sasaki, Kubota, Kajiwara & Shimada, 2002).

In the title compound, two kinds of In polyanions are contained in a monoclinic cell with a long a axis and a large unit-cell volume of 4588.6 (8) Å^3. There are 14 Ba atom sites, seven In atom sites and eight N atom sites in the asymmetric unit.

The arrangement of the atomic positions is shown in Fig. 1. N atoms are located in the centres of the Ba octahedra (Ba_6N). The interatomic distances between the N and Ba atoms are in the range 2.508 (12)–3.026 (9) Å, which is consistent with the

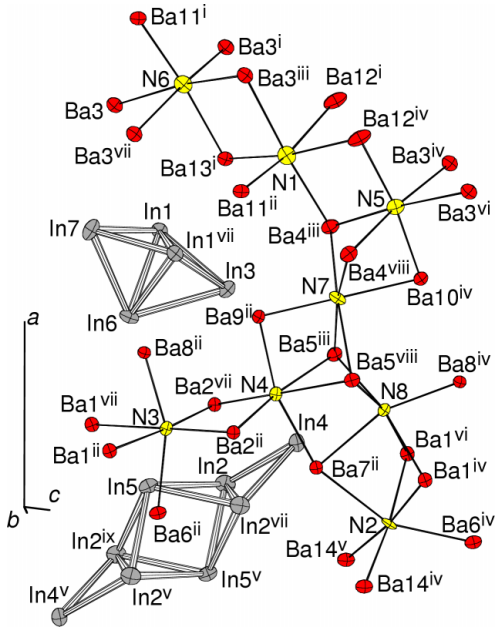

Figure 1
The arrangement of atomic positions in the structure of $Ba_{19}In_9N_9$, illustrated with 50% probability displacement ellipsoids. Symmetry codes as in Table 1.

Ba—N distances reported in the structure of $Ba_{14}Cu_2In_4N_7$ (2.46–3.07 Å; Yamane, Sasaki, Kubota, Kajiwara & Shimada, 2002). The bond-valence sums, calculated with the bond-valence parameters presented by Brese & O'Keeffe (1991), are 2.4 v.u. for N1 and range from 2.8 to 3.2 v.u. for the other seven N atoms.

Fig. 2 illustrates the crystal structure of $Ba_{19}In_9N_9$ with the nitrogen-centred Ba octahedra, which share edges and faces to form flat cages along the *c* axis. Polyanionic clusters with compositions of $[In_5]^{5-}$ and $[In_8]^{12-}$ are situated inside these cages. The structure of $Ba_{19}In_9N_9$ is thus represented by the formula $(Ba_{38}N_{18})[In_5]_2[In_8]$.

The trigonal–bipyramidal $[In_5]$ cluster consists of In atoms in In1, In3, In6 and In7 sites. The In—In distances range from 2.9569 (12) (In1—In3) to 3.224 (2) Å (In3—In6), which is in accordance with those reported for the indium Zintl compounds $Na_{15}In_{27.54}$, Na_2In (2.84–3.45 Å; Sevov & Corbett, 1993), $CaIn_2$ and $SrIn_2$ (2.91–3.27 Å; Iandelli, 1964). In $Ba_{19}In_9N_9$, In1 is surrounded by six Ba atoms, In3 by nine Ba atoms, and both In6 and In7 by eight Ba atoms, with In—Ba interatomic distances of 3.60–4.45 Å.

The trigonal–bipyramidal cluster $[In_5]$ has not been reported before, but square pyramids of $[In_5]$ were revealed for the Zintl compounds La_3In_5 and Y_3In_5 (Zhao & Corbett, 1995). The formal charge of the $[In_5]$ square pyramids is given as −9. In this kind of cluster, In—In distances of 3.00–3.23 Å are found. The interatomic distances between discrete $[In_5]$ square pyramids are 3.22–3.58 Å and the $[In_5]$ groups are linked to form Zintl network structures. These compounds exhibit metallic conduction. The trigonal–bipyramidal $[In_5]$ clusters in $Ba_{19}In_9N_9$ are surrounded by Ba atoms and are isolated from each other. Considering $[In_5]$ as a typical Zintl anion, the formal charge of the four-coordinated In1 and In6 is −1, that of the three-coordinated In3 and In7 is −2, and the total charge of the bipyramidal $[In_5]$ polyanion is −7. This is isoelectronic with the bipyramidal polyanions $[Ga_5^{7-}]$ found in the subnitrides Sr_6Ga_5N and Ba_6Ga_5N (Cordier *et al.*, 1995), the $[Tl_5^{7-}]$ polyanions in $Na_2K_{21}Tl_{19}$ (Dong & Corbett, 1994), and the $[Pb_5^{2-}]$ and $[Sn_5^{2-}]$ polyanions in $[cryptNa^+]_2[Pb_5^{2-}]$ and $[cryptNa^+]_2[Sn_5^{2-}]$ (Edwards & Corbett, 1977). Sr_6Ga_5N and Ba_6Ga_5N are better represented as $\{(M_6N^{9+})[Ga_5^{7-}] + 2e^-\}$, where *M* = Sr or Ba, and two electrons are in excess.

The $[In_8]$ cluster in $Ba_{19}In_9N_9$ has a unique structure that is composed of four In2, two In4 and two In5 atoms. The In—In distances are 2.969 (2)–3.102 (1) Å, and thus are in the range of the $[In_5]$ and other In polyanions observed in various subnitrides. The bonding between In5 atoms was not considered because of the long distance of 3.493 (2) Å. The distances between the In atoms of the $[In_8]$ cluster and surrounding Ba atoms are 3.604 (1)–4.161 (1) Å. Five Ba atoms are situated around In2, ten Ba atoms around In4, and six Ba atoms around In5.

Since atoms In2 and In5 are bonded to four In atoms, the formal charge of these In atoms is expected to be −1 from the simple octet principle of Zintl anions. On the other hand, atom In4 only bonds to two In2 atoms and is therefore expected to have a formal charge of −3. The resultant total formal charge of the $[In_8]$ polyanion becomes −12. However, the charge in $Ba_{19}In_9N_9$ is not balanced as $\{(Ba^{2+})_{38}(N^{3-})_{18}([In_5^{7-}])_2([In_8^{12-}]) - 4e^-\}$. A similar electron shortage was reported for Ba_8Ga_7: $\{(Ba^{2+})_8[Ga_4^{8-}][Ga_3^{9-}] - 1e^-\}$ (Fornasini, 1983). In the latter, each Ga atom has three bonds to the neighbouring Ga atoms and carries −2 charges in a tetrahedral $[Ga_4^{8-}]$ cluster. Ga^{3-} atoms form a triangular $[Ga_3^{9-}]$ cluster.

To obtain a deeper insight into the electronic structure of the $[In_8]$ and $[In_5]$ clusters and the related $[Ga_5]$ cluster, crystal overlap population analysis of these clusters was carried out by the DV-Xα method with the program *SCAT* (Adachi *et al.*, 1978). The bipyramidal $[Ga_5]$ cluster calculated with the atomic coordinates of Ba_6Ga_5N clearly showed that full occupation of the bonding molecular orbitals (MOs) causes the formal valence of −7 ($[Ga_5^{7-}]$), as expected from the Zintl principle. However, the $[In_5]$ cluster in $Ba_{19}In_9N_9$ can receive only five electrons in the bonding orbitals. The diffuse 4*d* orbitals of the In atoms seem to affect the bonding character of the $[In_5]$ cluster. If two more electrons entered in the next antibonding MO, the $[In_5]$ cluster would be unstable. Ten electrons from Ba atoms go into the bonding MOs of the $[In_8]$ cluster. The highest occupied MO of $[In_8^{12-}]$ is close to a non-bonding or slightly antibonding state. The core part of In2—In5 is bonding, but In2—In4 is antibonding in the HOMO. Thus a formal valence of −12 might be possible for the $[In_8]$ cluster and $Ba_{19}In_9N_9$ could be explained as $\{(Ba^{2+})_{38}(N^{3-})_{18}([In_5^{5-}])_2([In_8^{12-}])\}$.

Experimental

In an argon-filled glove box, Ba (99.99%), In (99.999%) and Na (99.95%), in a Ba:In:Na atomic ratio of 2:1:6, were weighed and loaded into a BN crucible (inside diameter 7 mm, height 37.5 mm and 99.5%). The crucible was placed into a stainless-steel container (0.5 inch outer diameter) and sealed with Ar gas. A schematic illustration of the stainless-steel container was given in a previous paper (Aoki *et al.*, 2000). The container was connected to an N_2 gas feed line. After heating to 1023 K in an electric furnace, N_2 gas (> 99.9999%) was introduced into the container and the pressure was maintained at 7 MPa with a pressure regulator. The sample was heated at this temperature for 1 h and then cooled to 823 K at a rate of 2 K h^{-1} under 7 MPa of N_2. Below 823 K, the sample was cooled to room temperature in the furnace by shutting off the furnace power. The products in the crucible were then washed in liquid NH_3 (99.999%) to dissolve the Na flux. The details of the Na extraction procedure were described previously (Kowach *et al.*, 1998). Single platelet crystals of $Ba_{19}In_9N_9$ with a black metallic lustre were obtained (maximum size 1.5 × 0.5 × 0.2 mm) together with crystals of $Ba_6In_{4.77}N_{2.7}$. The structures of $Ba_6In_{4.77}N_{2.7}$ and $Sr_6In_{4.3}N_{2.3}$ will be reported elsewhere (Bailey *et al.*, 2004). A scanning electron microscope (SEM, Jeol ISM-5400F), equipped with an energy dispersive X-ray spectrometer (EDS, Boyger), was used to evaluate the elemental composition for Ba and In in $Ba_{19}In_9N_9$. The EDS analysis showed the presence of Ba and In with an atomic ratio of Ba:In = 18.6–20.1:9, which agrees with the ideal ratio with respect to the formula $Ba_{19}In_9N_9$. Single crystals were selected from the reaction products in the glove box and were sealed in argon-filled glass capillaries since the crystals were not stable in air.

Crystal data

$Ba_{19}In_9N_9$	D_x = 5.456 Mg m^{-3}
M_r = 3768.93	Mo $K\alpha$ radiation
Monoclinic, $C2/m$	Cell parameters from 880 reflections
a = 57.334 (6) Å	θ = 3.1–29.1°
b = 7.9101 (8) Å	μ = 20.42 mm^{-1}
c = 10.1991 (10) Å	T = 293 (2) K
β = 97.237 (2)°	Plate, black
V = 4588.6 (8) Å^3	0.09 × 0.08 × 0.04 mm
Z = 4	

Data collection

Bruker SMART CCD area-detector diffractometer	7053 independent reflections
	5072 reflections with $I > 2\sigma(I)$
ω scans	R_{int} = 0.087
Absorption correction: analytical face-indexed (*XPREP*; Bruker, 1997)	θ_{max} = 30.0°
	$h = -57 \rightarrow 79$
	$k = -10 \rightarrow 11$
T_{min} = 0.186, T_{max} = 0.465	$l = -14 \rightarrow 13$
19 778 measured reflections	

Refinement

Refinement on F^2	$w = 1/[\sigma^2(F_o^2) + (0.0447P)^2]$ where $P = (F_o^2 + 2F_c^2)/3$
$R[F^2 > 2\sigma(F^2)]$ = 0.042	$(\Delta/\sigma)_{max}$ = 0.001
$wR(F^2)$ = 0.106	$\Delta\rho_{max}$ = 10.26 e Å^{-3}
S = 0.95	$\Delta\rho_{min}$ = −3.82 e Å^{-3}
7053 reflections	
198 parameters	

Table 1
Selected interatomic distances (Å).

N1—Ba13^{i}	2.663 (9)	N6—Ba3	2.954 (9)
N1—Ba11^{ii}	2.694 (9)	N6—Ba3^{vii}	2.954 (9)
N1—Ba4^{iii}	2.743 (10)	N7—Ba9^{ii}	2.576 (11)
N1—Ba12^{iv}	2.959 (9)	N7—Ba4^{viii}	2.672 (8)
N1—Ba3^{iii}	2.962 (10)	N7—Ba4^{iii}	2.672 (8)
N1—Ba12^{i}	3.026 (9)	N7—Ba10^{iv}	2.726 (11)
N2—Ba14^{v}	2.658 (7)	N7—Ba5^{iii}	2.881 (9)
N2—Ba14^{iv}	2.658 (7)	N7—Ba5^{viii}	2.881 (9)
N2—Ba1^{iv}	2.721 (7)	N8—Ba8^{iv}	2.563 (10)
N2—Ba1^{vi}	2.721 (7)	N8—Ba5^{viii}	2.644 (8)
N2—Ba6^{iv}	2.786 (11)	N8—Ba5^{iii}	2.644 (8)
N2—Ba7^{ii}	3.027 (12)	N8—Ba1^{vi}	2.817 (8)
N3—Ba8^{ii}	2.612 (11)	N8—Ba1^{iv}	2.817 (8)
N3—Ba2^{ii}	2.684 (7)	N8—Ba7^{ii}	2.820 (10)
N3—Ba2^{vii}	2.684 (7)	In1—In7	2.9552 (12)
N3—Ba6^{ii}	2.743 (11)	In1—In3	2.9569 (12)
N3—Ba1^{vii}	2.784 (8)	In1—In6	3.1147 (11)
N3—Ba1^{ii}	2.784 (8)	In1—In1^{vii}	3.1639 (14)
N4—Ba9^{ii}	2.606 (11)	In2—In2^{vii}	2.9685 (17)
N4—Ba2^{vii}	2.644 (7)	In2—In4	3.0090 (12)
N4—Ba2^{ii}	2.644 (7)	In2—In5^{v}	3.0565 (13)
N4—Ba7^{ii}	2.765 (11)	In2—In5	3.1021 (13)
N4—Ba5^{viii}	2.914 (8)	In2—In2^{ix}	4.1128 (17)
N4—Ba5^{iii}	2.914 (8)	In3—In1^{vii}	2.9569 (12)
N5—Ba10^{iv}	2.508 (12)	In3—In6	3.2243 (16)
N5—Ba12^{iv}	2.562 (12)	In4—In2^{vii}	3.0090 (12)
N5—Ba4^{iii}	2.799 (9)	In5—In2^{ix}	3.0564 (13)
N5—Ba4^{viii}	2.799 (9)	In5—In2^{v}	3.0564 (13)
N5—Ba3^{iv}	2.965 (9)	In5—In2^{vii}	3.1021 (13)
N5—Ba3^{vi}	2.965 (9)	In5—In5^{v}	3.493 (2)
N6—Ba11^{i}	2.635 (13)	In6—In1^{vii}	3.1147 (11)
N6—Ba3^{iii}	2.662 (8)	In6—In7	3.1312 (16)
N6—Ba3^{i}	2.662 (8)	In7—In1^{vii}	2.9552 (12)
N6—Ba13^{i}	2.825 (13)		

Symmetry codes: (i) $\frac{1}{2}-x,\frac{1}{2}-y,1-z$; (ii) $x,1+y,z$; (iii) $\frac{1}{2}-x,\frac{1}{2}+y,1-z$; (iv) $x,1+y,1+z$; (v) $-x,1-y,1-z$; (vi) $x,1-y,1+z$; (vii) $x,1-y,z$; (viii) $\frac{1}{2}-x,\frac{3}{2}-y,1-z$; (ix) $-x,y,1-z$.

The highest peak and deepest hole in the F_o–F_c map were observed at (0.0235, 0.5, 0.6884), 1.49 Å from In2, and at (0.0165, 0.2720, 0.6705), 0.49 Å from In2, respectively. The position of the highest peak is at the centre of the In2—In2^{vii} bond within the [In$_8$] cluster, and the deepest hole is close to the In2 atoms and outside the In2—In2^{vii} bond. Peaks of 2.2–3.9 e Å^{-3} were also observed at 0.71–0.96 Å distant from Ba atoms and from In6 and In7. These large differences are presumably a result of the cut-off effect of the Fourier synthesis in a low-symmetry space group with many heavy atoms in a large cell.

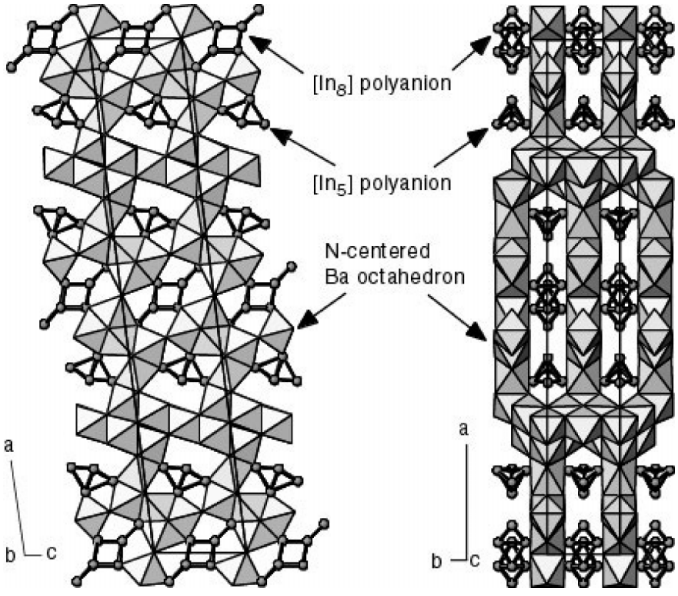

Figure 2
The structure of $Ba_{19}In_9N_9$ in projection along [010] (left) and along [001] (right), with N-centred Ba octahedra and In atoms shown as grey circles with bonds.

Data collection: *SMART* (Bruker, 1999); cell refinement: *SAINT* (Bruker, 1999); data reduction: *SAINT*; program(s) used to solve structure: *SIR*97 (Altomare *et al.*, 1999); program(s) used to refine structure: *SHELXL*97 (Sheldrick, 1997); molecular graphics: *ATOMS* (Dowty, 1999); software used to prepare material for publication: *SHELXL*97.

We thank Professor T. Ito for his encouragement and support. Useful discussions with M. S. Bailey are appreciated.

References

Adachi, H., Tsukada, M. & Satoko, C. (1978). *J. Phys. Soc. Jpn*, **45**, 875–883.
Altomare, A., Burla, M. C., Camalli, M., Cascarano, G. L., Giacovazzo, C., Guagliardi, A., Moliterni, A. G. G., Polidori, G. & Spagna, R. (1999). *J. Appl. Cryst.* **32**, 115–119.
Aoki, M., Yamane, H., Shimada, M., Sekiguchi, T., Hanada, T., Yao, T., Sarayama, S. & DiSalvo, F. J. (2000). *J. Cryst. Growth*, **218**, 7–12.
Bailey, M. S. *et al.* (2004). In preparation.
Brese, N. E. & O'Keeffe, M. (1991). *Acta Cryst.* B**47**, 192–197.
Bruker (1997). *XPREP* in *SHELXTL* (Version 6.02A). Bruker AXS Inc. Madison, Wisconsin, USA.
Bruker (1999). *SMART* (Version 5.611) and *SAINT* (Version 6.02A). Bruker AXS Inc. Madison, Wisconsin, USA.
Cordier, G., Ludwig, M., Stahl, D., Schmidt, P. C. & Kniep, R. (1995). *Angew. Chem. Int. Ed. Engl.* **34**, 1761–1763.
Cordier, G. & Rönninger, S. (1987). *Z. Naturforsch. Teil B*, **42**, 825–827.
Dong, Z. & Corbett, J. D. (1994). *J. Am. Chem. Soc.* **116**, 3429–3435.
Dowty, E. (1999). *ATOMS.* Shape Software, 521 Hidden Valley Road, Kingsport, TN 37663, USA.
Edwards, P. A. & Corbett, J. D. (1977). *Inorg. Chem.* **16**, 903–907.
Fornasini, M. L. (1983). *Acta Cryst.* C**39**, 943–946.
Iandelli, A. (1964). *Z. Anorg. Allg. Chem.* **330**, 221–232.

Kowach, G. R., Lin, H. Y. & DiSalvo, F. J. (1998). *J. Solid State Chem.* **141**, 1–9.
Sevov, S. C. & Corbett, J. D. (1993). *J. Solid State Chem.* **103**, 114–130.
Sheldrick, G. M. (1997). *SHELXL*97. University of Göttingen, Germany.
Yamane, H., Sasaki, S., Kubota, S., Inoue, R., Shimada, M. & Kajiwara, T. (2002). *J. Solid State Chem.* **163**, 449–454.
Yamane, H., Sasaki, S., Kubota, S., Kajiwara, T. & Shimada, M. (2002). *Acta Cryst.* C**58**, i50–i52.
Yamane, H., Sasaki, S., Kubota, S., Shimada, M. & Kajiwara, T. (2003). *J. Solid State Chem.* **170**, 265–272.
Zhao, J.-T. & Corbett, J. D. (1995). *Inorg. Chem.* **34**, 378–383.